Electronic Journal of Structural Engineering

Original Article

Cite this: DOI:10.56748/ejse.25712

Received Date: 21 November 2024
Accepted Date: 22 February 2025

1443-9255
https://ejsei.com/ejse

Evaluation of Parameters Affecting the Inelastic Acceleration Ratio

Emad A. Elhout [a]*

[a] Associate Professor, Civil Engineering Department, Faculty of Engineering, Damanhour University, Egypt
*Corresponding author: emad_aliali@yahoo.com

Abstract

The Inelastic Acceleration Ratio (IAR) is a helpful instrument for determining the maximum inelastic acceleration from the related elastic acceleration that seems to have been little examined in past research. The IARs using single-degree-of-freedom (SDOF) systems with various structural factors under thirty pairs of ground motion earthquakes recorded are investigated in this paper. The linear elastic-perfect plastic model is used to model SDOF systems. The factors to consider include elastic vibration period (T), displacement ductility ratios (μ, 2-8), the post-yield stiffness ratio (α, 0-15%), and the damping ratio (ξ, 3-20%). The results showed that the IAR values decreased with an increase in the ductility ratios (μ) while the IAR values are increased with an increase in the damping ratios (ξ). While the post-yield stiffness ratio (α) has little effect on the IAR. Also, Analytical formulae are used to estimate IAR based on the T, μ, α, and ξ.

Keywords

Inelastic acceleration ratio, Damping ratio, Post-yield stiffness ratio, Vibration period, Ductility ratio, Inelastic displacement ratio, Inelastic velocity ratio

1. Introduction

Many studies are focused on evaluating the inelastic seismic response of building structures. This remains one of the most significant problems in structural engineering. So, the seismic performance evaluation of nonlinear structure analysis must be evaluated accurately to define the structure's reliable earthquake resistance. The seismic design of structures reduces collapse by allowing structural components to distribute seismic energy through inelastic deformations. Most studies use linear analysis using some parameters to predict the nonlinear responses of structures under seismic loads, such as using the inelastic spectra through parameters based on their elastic responses. The Inelastic Displacement Ratios (IDRs), Inelastic Velocity Ratios (IVRs), and Inelastic Acceleration Ratios (IARs) allow the computation of maximum inelastic displacements, velocities, and accelerations, respectively, without performing complicated inelastic analyses, direct from the equivalent elastic ones.

The maximum lateral displacement always predicted seismic design codes to evaluate the seismic demand of structure under earthquake based on elastic response spectrum which is based on the IDRs. The IDR is the SDOF system's maximum inelastic to maximum elastic displacement ratio. This factor has been used in prior investigations for achieving inelastic displacement without requiring nonlinear dynamic analysis. Hatzigeorgiou and Beskos, 2009 presented a simple method to estimate the IDR of a structure under repeated or multiple earthquakes. Many parameters such as damping ratio, local site conditions, post-yield stiffness ratio, force reduction factors and the structural period of vibration are taken to find expressions for this ratio. It was found that the viscous damping ratio and local site conditions are not significantly affected in estimating the IDRs. The post-yield stiffness ratio, force reduction factors, and the structural period of vibration are influences on estimating the IDR.

Ruiz-García, 2011 evaluated the IDR of SDOF systems subjected to near-fault ground motions. Also, an estimated equation to obtain the IDR for the seismic assessment of structures exposed to forward-directivity near-fault ground motions is proposed. The IDR of nonstructural components that were subjected to floor accelerations was examined by Obando and Lopez-Garcia, 2016. Chimneys, cooling systems, antennae, and barriers are some acceleration-sensitive nonstructural elements where the inelastic displacement demand is relevant. Chikh et al. 2017 estimated the IDR for SDOF bilinear systems by rigorous nonlinear analysis which depends on the period, the post-to-pre-yield stiffness ratio, the yield strength reduction factor, and the peak ground acceleration. De Francesco, 2019 study the constant-ductility IDR of SDOF systems with two different levels of energy dissipation capacity, in the presence of a 5% viscous damping ratio. The research includes 228 ground motions with magnitudes larger than six that were observed in California. The behavior of self-centering SDF systems with many parameters is studied and compared to those of SDF systems with bilinear plastic. The analysis indicated that Like in all the other hysteretic systems studied, the dispersion in the earthquake data is the number of inelastic displacement ratios of self-centering systems based on the aggregate effects of ductility, starting period, and post-yield stiffness ratio.

Yaghmaei-Sabegh et al. 2020 estimated the IDR of SDOF systems with damping ratios and post-yield stiffness ratios in underground motion records obtained at sites of soft soil. As a function of numerous parameters, a simplified equation has also been suggested through the use of nonlinear regression analysis. It can be concluded that the effect of soil condition on the inelastic displacement ratio increases with increasing ductility level and the damping ratio. Dong et al. 2020 investigated the IDR of SDOF systems to the self-centering structure subjected to near- and far-fault ground motions. Different parameters such as ductility levels, peak ground velocity, site condition, and the natural period are used in this study. The results indicated that the post-yielding stiffness ratio, energy dissipation ratio, ductility factor, and vibration period have a significant effect on the inelastic displacement ratio. Moreover, a flag-shaped model has more effect on the inelastic displacement demands of the structure than the bilinear model and Modified Clough model. Additionally, a simplified formula is created to determine the IDR for self-centering structure design. Applying information regarding the IDR of SDOF systems with strength and stiffness degraded peak-oriented hysteretic theory and failure threat through nonlinear time history evaluations, BÖREKÇİ and AYDOĞAN, 2024 provided Artificial Neural Network models. The results show that, for a given set of parameters, Artificial Neural Network approaches produce higher precision than earlier techniques and may be implemented for calculating the IDR. As has already been indicated, a thorough analysis of the IDR's review has been done in the past. Another way to seismically protect the structure's inelastic yielding is to install isolation devices or dampers at the base (Soni et al. 2011 and Piasal et al. 2016)

However, there hasn't been much research done on determining velocities for inelastic constructions that are exposed to severe earthquakes. It seems that evaluating velocities is important for many velocity-dependent nonlinear structures, especially inelastic constructions that have additional viscous dampers (FEMA450, and Kam et al. 2010). The ratio of the SDOF system's highest inelastic velocity to its maximum elastic velocity is known as the inelastic velocity ratio (IVR), according to Hatzigeorgiou and Papagiannopoulos, 2012. In addition to the equations for IVR as a function of the period of motion, damping ratio, force reduction factor, and soil type have been determined using substantial statistical research. A straightforward model utilizing the IVR was presented by Hatzigeorgiou and Pnevmatikos, 2014 for the assessment of effective velocities and damping forces for SDOF structures with additional viscous dampers during earthquakes. Under a dozen pulses record, Konstandakopoulou and Hatzigeorgiou, 2020 examined the constant-ductility inelastic spectra ratios for SDOF systems. According to the analysis, the type of pulse and the number of cycles affect the IDR, IVR, and IAR. Designers can assess the inelastic behavior of constructions by directly computing the highest inelastic acceleration using the equivalent elastic one using the IAR, which is another helpful index.

An additional third ratio related to acceleration is the inelastic response ratio (IAR), defined as the ratio between the maximum inelastic accelerations and its elastic ones. This parameter is utilized to assess the

seismic response of non-structural elements such as architectural, mechanical, electrical and plumbing elements that are acceleration-sensitive components under earthquake ground motions (Pardalopoulos and Pantazopoulou, 2015). The inelastic acceleration ratio (IAR) was studied by Garakaninezhad and Amiri, 2022 along with the influence of structural characteristics on this measure. These parameters include the elastic vibration period normalized by the pulse period, the strength modification factor, the viscous damping ratio, and the hysteretic principle. The chosen dataset contains ninety-one records of earthquakes. Moreover, mathematical formulas for estimating IAR due to the principal structural parameters and the normalized elastic vibration period are presented. These formulas can be utilized for the seismic assessment of non-structural and acceleration-sensitive buildings.

The IAR parameters did not examine a lot in much research for evaluating the inelastic buildings under seismic ground motion. So, the study aims to evaluate parameters affecting the inelastic acceleration ratio (IAR) of SDOF systems. Additionally, it would be beneficial to explore the real-world applications of IAR when it comes to the seismic design of structures. The IARs using SDOF systems with various structural factors under thirty pairs of ground motion earthquakes recorded are investigated in this paper. The linear elastic-perfect plastic model is used to model SDOF systems. The factors to consider include elastic vibration period (T), displacement ductility ratios (μ, 2-8), the post-yield stiffness ratio (α, 0-15%), and the damping ratio (ξ, 3-20%). Also, analytical formulae are provided to estimate IAR as a function of T, μ, α, and ξ. This can be used to investigate the seismic performance of acceleration-sensitive structures and parts that are not structural.

2. Inelastic Acceleration Ratio (IAR)

The IAR (μ, T) is defined for constant-ductility inelastic spectra as the ratio between the maximum inelastic spectra accelerations and its elastic ones [15]:

$$IAR\ (\mu,T) = \frac{SA(\mu,T)}{SA(\mu=1,T)} \qquad (1)$$

This paper evaluates IARs using SDOF systems with a variety of structural factors. The factors to consider include elastic vibration period (T), displacement ductility ratios (μ), and the damping ratio (ξ). The seismic elastic response spectra were obtained at the site of interest using the calculated technique criteria. It applies all dynamic properties of the soil layers through modeling using a finite element approach procedure, and it employs the same seismic hazard maps to generate simulations of compatible synthetic accelerograms.

In this study, the software SeismoSignal version 4.3.0 determines the elastic and inelastic spectrum accelerations to all earthquake records. Strong-motion data can be developed in an efficient and casual manner with the help of this application. Additionally, it is adept at descending a variety of strong-motion characteristics that are frequently needed by earthquakes and seismologists.

The examination of all the records of an earthquake has been carried over 400 separate periods that go from 0.02 to 4.0 seconds. varieties of nonlinear spectra for each ground motion earthquake are calculated. The linear elastic-perfect plastic model is used to model SDOF systems, and the post-yield stiffness ratio is set to 0%, 5%, 10%, and 15%. The displacement ductility ratios (μ) used are 2, 4, 6, and 8. Consider damping ratios (ξ) of 3%, 5%, 10%, and 20%. The plotted spectrum for each ductility ratio, and damping ratios for all horizontal ground motion earthquake records are calculated.

3. Database of Strong Motions Earthquake Records

This study's analysis used thirty pairs of ground motion earthquakes recorded between 1971 and 1999 from the COSMOS Virtual Data Centre to a wide range of closest distances and seismic moment magnitudes (COSMOS, 2017). The earthquakes at the closest distance range from 2.31 to 106.8 km, the PGA (g) of the earthquake records is between 0.02 and 1.5 and the moment magnitudes range from 5.2 to 7.5 as shown in figures (1 and 2). Table 1 presents the earthquake records and the associated data.

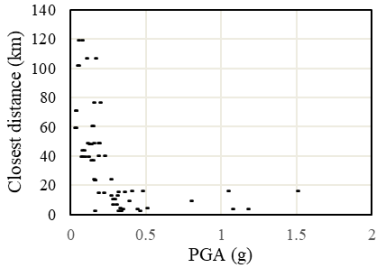

Fig. 1 The relation between closest distance and PGA (g) of ground motion records.

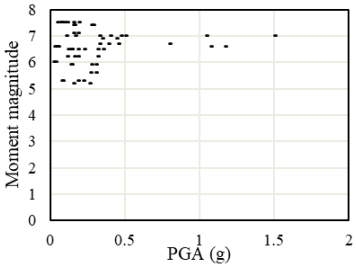

Fig. 2 The relation between the moment magnitude and PGA (g) of ground motion records.

4. Inelastic Acceleration Ratio (IAR)

The IAR parameters obtained by the dynamic nonlinear analysis based on ground motion information are presented in the next subsection. The linear elastic-perfect plastic model is used to model SDOF systems, and the post-yield stiffness ratio (α) is set to 0.0, 0.05, 0.1, and 0.15. The displacement ductility ratios (μ) used are 2, 4, 6, and 8. The damping ratios (ξ) are used at 3%, 5%, 10%, and 20%.

4.1 Variation of the mean IAR with the ductility ratio (μ)

The mean IAR -T spectra evaluated for this study's thirty pairs of ground motions as shown in Fig. 3. The spectra show SDOFs with ξ = 5%, varying ductility ratios (μ=2, 4, 6, and 8) and post-yield stiffness ratios (α = 0.0, 0.05, 0.1, and 0.15). The results show that μ considerably impacts a considerable impact on the mean IAR. Increasing μ causes a decrease in IAR over a given period. These results are consistent with Konstandakopoulou and Hatzigeorgiou, 2020.

Fig. 3 further shows that the mean IAR is significantly reliant on T in the short-period region of 0 to 0.1 seconds for all α levels. The spectrum seems to be a sequence of straight lines in this region. However, for periods greater than 0.1 seconds, the mean IAR is roughly period independent. IAR has shown a general tendency to increase as the period of the systems increases for periods greater than 0.1 sec and these results are consistent with Konstandakopoulou and Hatzigeorgiou, 2020. Also, the mean IAR is significantly increasing by increasing α, especially for high ductility ratio.

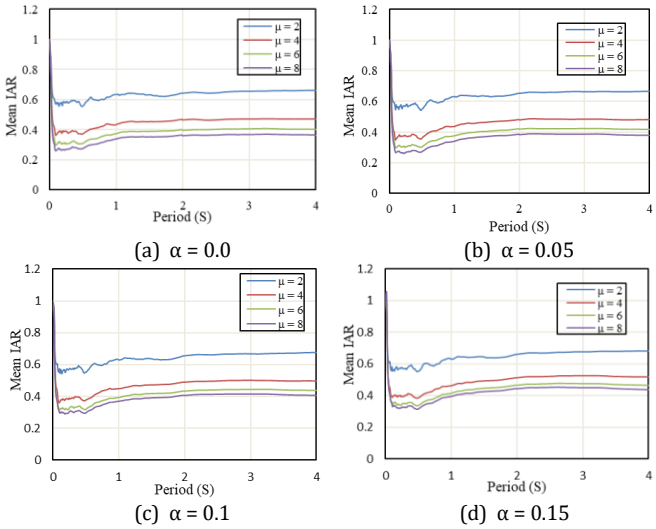

Figure 3 The mean IAR varies with μ for SDOFs with varying α and 5% damping.

Table 1. Data of earthquake records

NO	Earthquake name	Year	Station Name	Moment magnitude	Closest distance (km)	Site Geology	Com	A (g)	V (m/sec)
1	Joshua Tree/Hector Mine	1999	Amboy	7.1	48.4	Alluvium	360	0.149	0.19
							90	0.182	0.27
2	Redding	1998	Redding, CA	5.2	24	-	90	0.26	0.094
							360	0.148	0.035
3	Northridge	1994	Saticoy ST	6.7	2.31	-	S00E	0.453	0.61
							S90E	0.325	0.31
4	Northridge	1994	Sylmar - 6-Story County Hospital	6.7	8.7	Alluvium	90	0.383	0.71
							0	0.797	11.2
5	Big Bear	1992	Desert Hot Springs	6.5	40.1	Deep Alluvium	360	0.18	0.16
							90	0.22	0.19
6	Cape Mendocino	1992	Cape Mendocino, CA – Petrolia	7.0	15.5	Cretaceous Rock	90	1.04	0.41
							0	1.5	1.26
7	Landers	1992	Joshua Tree	7.4	10	Alluvium	0	0.273	0.27
							90	0.283	0.42
8	Landers	1992	Pomona	7.5	118.7	Alluvium	90	0.044	0.085
							0	0.067	0.12
9	Landers	1992	Desert Hot Springs	7.4	23.1	Deep Alluvium	90	0.153	0.2
							150	0.156	0.12
10	Petrolia	1991	Eureka - Myrtle & West Avenue	6	59.1	Partly Cons Sediments	360	0.02	0.03
							90	0.028	0.02
11	Limon, Costa Rica	1991	San Jose – Guatuso	7.5	39.4	-	0	0.11	0.09
							270	0.07	0.06
12	Limon, Costa Rica	1991	San Isidro	7.5	76.1	Alluvium	270	0.15	0.09
							0	0.188	0.14
13	Limon, Costa Rica	1991	Puriscal	7.5	39.4	Alluvium	0	0.09	0.075
							270	0.066	0.076
14	Sierra Madre	1991	Cogswell Dam	5.6	12.6	weathered granitic rock	155	0.302	0.14
							65	0.264	0.096
15	Santa Cruz	1989	OLEMA	7.0	106.8	Alluvium	90	0.1	0.16
							0	0.161	0.18
16	Santa Cruz Mtns	1989	Capitola - Fire Station	7.0	15.9	Alluvium	90	0.398	0.30
							0	0.472	0.36
17	Santa Cruz Mtns	1989	Saratoga - Aloha Ave.	7.0	4.1	Alluvium	0	0.5	0.41
							90	0.322	0.44
18	Whittier Aftershock	1987	Tarzana - Cedar Hill Nursery	5.3	43.6	Alluvium	90	0.08	0.04
							0	0.071	0.029
19	Whittier Aftershock	1987	Fremont School	5.3	14.8	Alluvium	270	0.214	0.085
							180	0.178	0.1
20	Palm Springs	1986	Desert Hot Springs	5.9	6.8	Deep Alluvium	0	0.3	0.33
							90	0.273	0.18
21	Palm Springs	1986	Hemet - Stetson Ave Fire Station	5.9	36.9	Deep alluvium	360	0.14	0.05
							270	0.13	0.048
22	Morgan	1984	Halls Valley	6.2	2.5	Alluvium	240	0.312	0.396
							150	0.156	0.126
23	Coalinga	1983	Parkfield, CA - Cholame 5W	6.5	60.2	Sandstone	270	0.14	0.106
							360	0.136	0.107
24	Mammoth Lakes	1980	Benton	6.2	48.5	Alluvium	360	0.18	0.11
							270	0.106	0.072
25	Imperial Valley	1979	Coachella Canal Number 4	6.5	47.6	stiff soil	S45E	0.13	0.15
							N45E	0.116	0.12
26	Imperial Valley	1979	Huston Rd., El Centro Array #6, Ca	6.9	3.5	alluvium; more than 300m	S50W	0.437	1.13
							S40E	0.34	0.66
27	Friuli-Italy-01	1976	Tolmezzo	6.5	15.8		0	0.35	31
							270	0.31	30
28	San Fernando	1971	Pacoima Dam, Cal.	6.6	3.5	Highly joined Diorite Gneiss	S16E	1.17	1.135
							S74W	1.07	0.576
29	San Fernando	1971	Port Hueneme, Navy Laboratory, Cal.	6.6	70.8	Alluvium	S90W	0.03	0.06
							S00W	0.026	0.072
30	San Fernando	1971	San Bernardino, Cal	6.6	101.6	Alluvium	N00E	0.04	0.035
							N90E	0.045	0.027

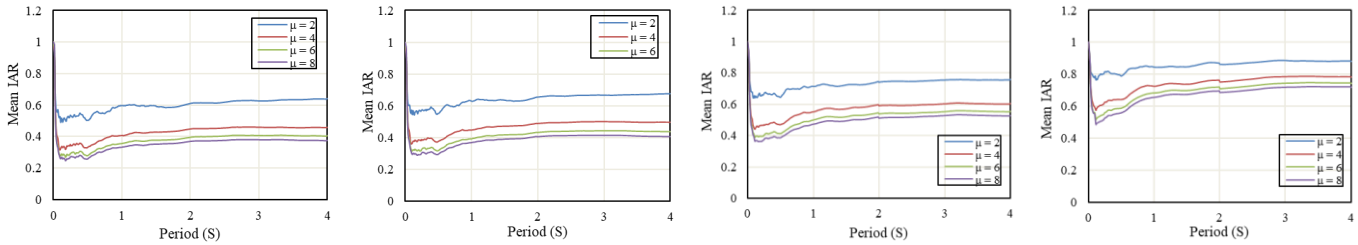

(a) ξ= 3% (b) ξ= 5% (c) ξ=10% (d) ξ= 20%

Fig. 4 The mean IAR varies with μ for SDOFs with varying ξ and with α equals to 0.1.

Fig. 4 shows the mean IAR -T spectra for SDOFs with post-yield stiffness ratio α equal to 0.1 and different ductility ratios (μ = 2, 4, 6, and 8) and damping ratios (ξ = 3%, 5%, 10%, and 20%). Fig. 4 shows results that are consistent with those in Fig. 3. The mean IAR is dependent on T in the short-period range and increasing the μ causes a decrease in IAR over a given period. The spectrum seems to be a sequence of straight lines in this region. The results show that the ξ considerably a considerable impact on the mean IAR. Increasing the ξ causes an increase in IAR over a given period for all values of μ. These results are consistent with the results of Konstandakopoulou and Hatzigeorgiou, 2020.

4.2 The Variation of the mean IAR with the post-yield stiffness ratio (α)

The mean IAR -T spectra evaluated for this study's thirty pairs of ground motions as shown in Fig. 5. The show SDOFs with ξ = 5%, varying ductility ratios (μ=2, 4, 6, and 8), and post-yield stiffness ratios (α = 0.0, 0.05, 0.1, and 0.15). The results show that the mean IAR is independent of α, especially for SDOFs with low ductility ratios. The α has a significant impact on mean IAR for SDOFs with large ductility ratios and periods longer than 0.1 sec.

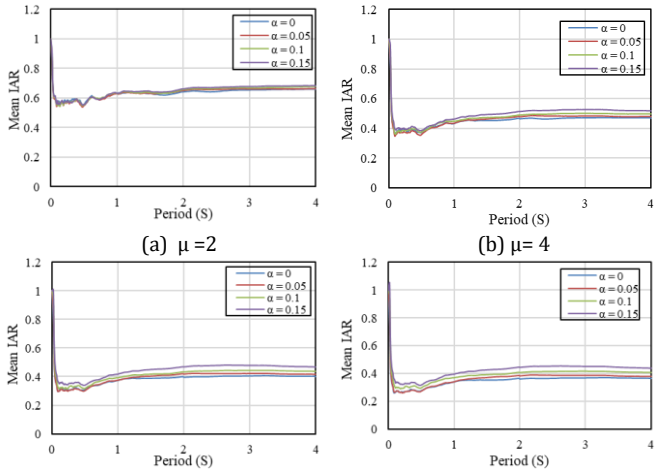

(a) μ =2 (b) μ= 4

(c) μ=6 (d) μ= 8

Fig. 5 The mean IAR varies with α for SDOFs with varying μ with ξ equals 5%.

The mean IAR -T spectra evaluated for this study's thirty pairs of ground motions as shown in Fig. 6. The spectra show SDOFs with μ equal to 6, varying damping ratios (ξ= 3%, 5%, 10%, and 20%), and post-yield stiffness ratios (α = 0.0, 0.05, 0.1, and 0.15). The results presented in Fig.10 indicate that the mean IAR is roughly independent of the α in cases of SDOFs with ξ= 10%, and 20%. The effect of the stiffness ratio α on the mean IAR is only pronounced for SDOFs with ξ= 3% and 5%. The study found that for SDOFs with high damping ratios, the mean IAR is mostly independent of α. The α has a significant impact on mean IAR for SDOFs with low damping ratios in periods longer than 0.1 sec. Figs. 5 and 6 show that the effect of α on mean IAR is only significant for SDOFs with low ductility ratios and high damping ratios. In SDOFs with high ductility ratios and low damping ratios, increasing the α leads to a rise in the mean IAR.

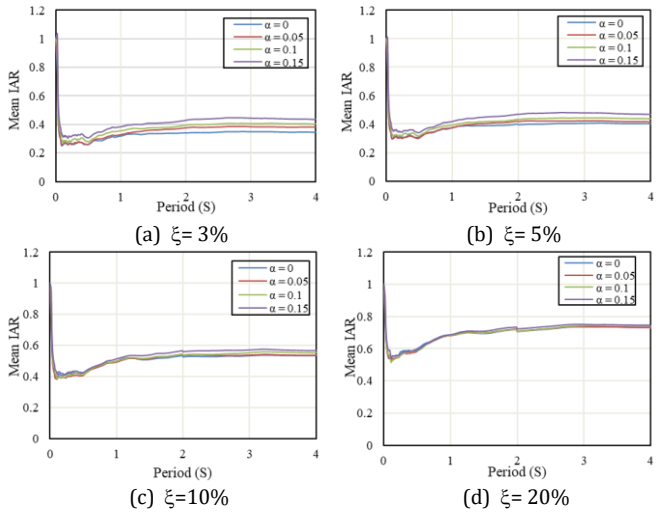

(a) ξ= 3% (b) ξ= 5%

(c) ξ=10% (d) ξ= 20%

Fig. 6 The mean IAR varies with α for SDOFs with varying ξ and with μ equal to 6.

4.3 The Variation of the mean IAR with the viscous damping ratio (ξ)

The mean IAR -T spectra evaluated for this study's thirty pairs of ground motions as shown in Fig. 7. The spectra show SDOFs with α equal to 0.1, varying damping ratios (ξ = 3%, 5%, 10%, and 20%,) and ductility ratios (μ = 2, 4, 6, and 8). Fig. 7 shows that ξ affect the mean IAR value. The ξ have a greater impact on the mean IAR in SDOFs with high ductility ratios. Increasing ξ leads to an increase in IAR over time, regardless of ductility ratio (μ).

The results show that the mean IAR is relatively independent of ξ, especially for SDOFs with periods shorter than 0.1 sec. The spectrum seems to be a sequence of straight lines in this region. Damping ratios (ξ) have a significant impact on mean IAR for SDOFs with ductility ratios lasting more than 0.1 second.

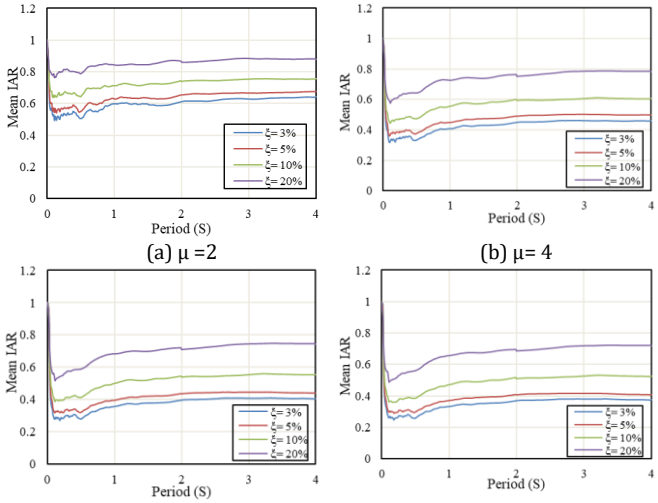

(a) μ =2 (b) μ= 4

(c) μ=6 (d) μ= 8

Fig. 7 The mean IAR varies with ξ for SDOFs with varying μ and with α equal to 0.1.

The mean IAR -T spectra evaluated for this study's thirty pairs of ground motions as shown in Fig. 8. The spectra show SDOFs with μ equal to 6, varying damping ratios (ξ= 3%, 5%, 10%, and 20%), and the post-yield stiffness ratio (α = 0.0, 0.05, 0.1, and 0.15). Fig. 8's results are consistent with those shown in Fig. 7. The ξ is an effect on the mean IAR of the SDOF system that the mean IAR is increased by increasing the ξ for all stiffness ratio α levels.

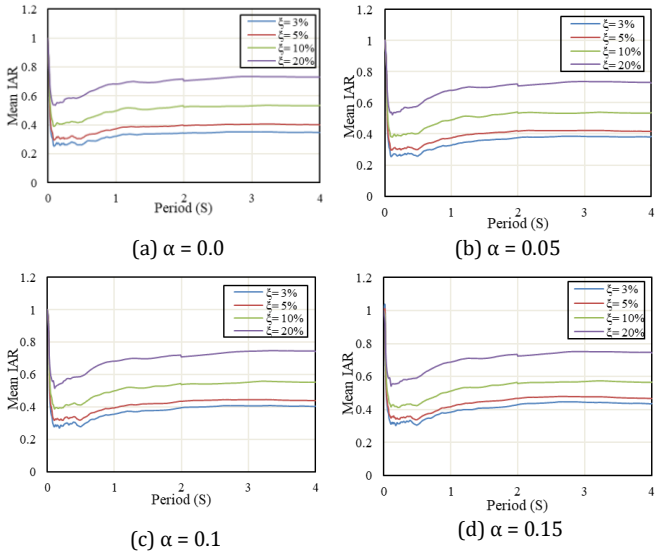

(a) α = 0.0 (b) α = 0.05

(c) α = 0.1 (d) α = 0.15

Fig. 8 The mean IAR varies with ξ for SDOFs with varying α and with μ equals 6.

5. Prediction Equations of IAR

For each SDOF system evaluated in this investigation, an individual mean IAR value is determined by the average mean IAR values over periods of less than 0.10 sec and longer than 0.1 sec. Tables 2 and 3 represent the mean IAR for SDOFs with varying α, ε, and μ values for periods less than 0.10 sec and higher than 0.1 sec, respectively.

Table 2. Mean IAR of SDOF systems having different α, ξ, and μ along the period less than 0.10 sec.

	ξ =3%				ξ= 5%				ξ= 10%				ξ= 20%			
α	μ= 2	μ= 4	μ= 6	μ= 8	μ= 2	μ= 4	μ= 6	μ= 8	μ= 2	μ= 4	μ= 6	μ= 8	μ= 2	μ= 4	μ= 6	μ= 8
0.0	0.601	0.437	0.379	0.347	0.641	0.477	0.417	0.382	0.715	0.557	0.495	0.459	0.817	0.674	0.611	0.581
0.05	0.595	0.438	0.391	0.367	0.631	0.472	0.423	0.398	0.706	0.546	0.491	0.464	0.813	0.664	0.610	0.585
0.10	0.598	0.458	0.423	0.413	0.635	0.493	0.457	0.444	0.704	0.556	0.514	0.498	0.806	0.661	0.618	0.604
0.15	0.608	0.485	0.462	0.460	0.643	0.517	0.492	0.488	0.709	0.578	0.548	0.541	0.807	0.675	0.646	0.639

Table 3. Mean IAR of SDOF systems having different α, ξ, and μ along the period greater than 0.10 sec.

	ξ=3%				ξ= 5%				ξ= 10%				ξ= 20%			
α	μ= 2	μ= 4	μ= 6	μ= 8	μ= 2	μ= 4	μ= 6	μ= 8	μ= 2	μ= 4	μ= 6	μ= 8	μ= 2	μ= 4	μ= 6	μ= 8
0.0	0.589	0.398	0.332	0.295	0.635	0.451	0.385	0.348	0.728	0.569	0.509	0.476	0.859	0.745	0.697	0.669
0.05	0.599	0.417	0.355	0.323	0.638	0.458	0.396	0.363	0.728	0.568	0.509	0.478	0.860	0.745	0.697	0.670
0.10	0.601	0.430	0.377	0.351	0.642	0.471	0.416	0.388	0.729	0.573	0.519	0.492	0.859	0.747	0.701	0.676
0.15	0.613	0.455	0.409	0.388	0.650	0.492	0.444	0.421	0.733	0.584	0.537	0.514	0.861	0.751	0.709	0.687

Table 4. Proposed IAR equations

NO.	Cases	Equations	(R^2)
1	T ≤ 0.10 sec	*IAR = 0.9 -5.31(T) – 0.03(μ) +0.0107(ξ) + 0.004(α)*	0.76
2	T > 0.10 sec	*IAR = 0.497 +0.029 (T) – 0.038(μ) +0.018 (ξ) + 0.002 (α)*	0.92

The following part provides the IAR's prediction formulas. Mathematical formulae for predicting the IAR of SDOF systems under 30 pairs of ground motion earthquakes using the linear elastic-perfect plastic model have been provided as an expression of T, μ, α, and ξ. The results presented two equations, the first to determine the IAR for the period structural systems less than 0.10 sec., and the second for the period structural systems greater than 0.10 sec. Table 4 summarizes all the suggested formulas.

Where, T= the elastic vibration period, μ = displacement ductility ratios, α = the post-yield stiffness ratio, and ξ= the damping ratio. Fig. 9 shows Konstandakopoulou and Hatzigeorgiou's, 2020 estimated IAR results to the suggested IAR equations produced in the current research for various α, ξ and μ values. Konstandakopoulou and Hatzigeorgiou's, 2020 [15] IAR is consistent with the suggested formulas for various α, ξ and μ values.

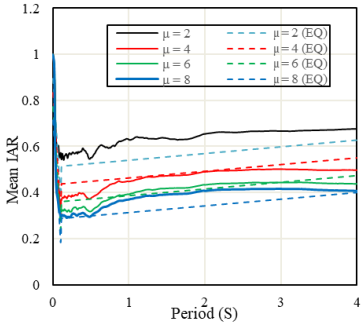

(a) The mean IAR varies with μ for SDOFs with ξ = 5% and α = 0.1

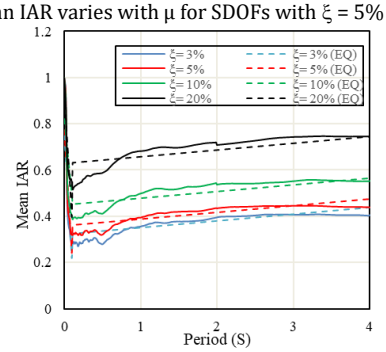

(b) The mean IAR varies with ξ for SDOFs with μ = 6 and α = 0.1.

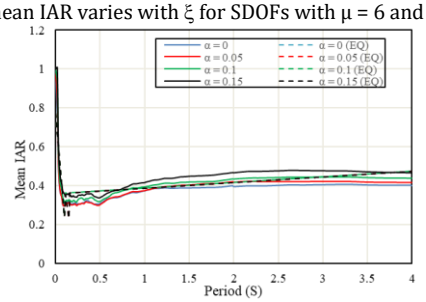

(c) The mean IAR varies with α for SDOFs with ξ = 5% and μ = 6

Fig. 9 Proposed IAR equations

6. Conclusions

This study aims to evaluate the IAR of SDOF systems with a variety of structural factors under thirty pairs of ground motion earthquakes recorded. The linear elastic-perfect plastic model is used to model SDOF systems. The factors to consider include elastic vibration period (T), displacement ductility ratios (μ, 2-8), the post-yield stiffness ratio (α, 0-15%), and the damping ratio (ξ, 3-20%). According to the outcomes derived from this research's evaluations, the results that follow can be reached:

(1) The post-yield stiffness ratio (α) has little effect on the IAR.
(2) The IAR values decrease with an increase in the ductility ratios (μ) over a given period for all values of the damping ratios (ξ) and all post-yield stiffness ratio (α) levels.
(3) The IAR values are increased with an increase in the damping ratios (ξ) over a given period for all values of the ductility ratios (μ) and all post-yield stiffness ratio (α) levels.
(4) The mean IAR is significantly reliant on T in the short-period region of 0 to 0.1 seconds for all stiffness ratio (α) levels.
(5) The mean IAR has shown a general tendency to increase as the period of the systems increases for periods greater than 0.1 sec.
(6) The IAR determined by Konstandakopoulou and Hatzigeorgiou (2020) agrees with the presented equations for various α, ξ, and μ levels.

The conclusions of this study rely on pairs of thirty ground motion earthquakes to calculate IAR, thus it is worth noting. More research on the effect of additional ground motion earthquake characteristics such as the PGA/PGV ratio, soil type, and earthquake magnitude levels on IAR. Additionally, it would be beneficial to explore the real-world applications of IAR when it comes to the seismic design of structures.

References

BÖREKÇİ, M., and AYDOĞAN, B. "Prediction of inelastic displacement ratios for evaluation of degrading SDOF systems: A comparison of the scaled conjugate gradient and Bayesian regularized artificial neural network modeling", Sigma Journal of Engineering and Natural Sciences, Vol. 42(1), 2024, pp 211-224. https://doi.org/10.14744/sigma.2024.00018

Chikh, B., Ahmed, M., Nacer, L., Moussa, L., Youcef, M., Mohamed, H., Abderrahmane, K., Djilali, B. "Seismic structural demands and inelastic deformation ratios: a theoretical approach", Earthquakes and Structures, Vol.12 (4), 2017, pp 397-407. https://doi.org/10.12989/eas.2017.12.4.397

COSMOS, The Consortium of Organizations for Strong-Motion Observation Systems, 2017. http:// www.cosmos-eq.org/

De Francesco, G. "Constant-ductility inelastic displacement ratios for displacement-based seismic design of self-centering structures", Earthquake Engineering Structure Dynamic, Vol. 48, 2019, pp188–209. https://doi.org/10.1002/eqe.3131

Dong, H., Han, Q., Du, X., Liu, J. "Constant ductility inelastic displacement ratios for the design of self-centering structures with flag-shaped models subjected to pulse-type ground motions", Soil Dynamics and Earthquake Engineering, Vol. 133, 2020, pp 106143. https://doi.org/10.1016/j.soildyn.2020.106143

Federal Emergency Management Agency- FEMA450, NEHRP Recommended Provisions for Seismic Regulations for New Buildings and Other Structures, Part 1: Provisions and Part 2: Commentary, Washington D.C, 2023.

Garakaninezhad A., Amiri, S. "Inelastic acceleration ratio of structures under pulse-like earthquake ground motions", In Structures, Vol. 44, 2022, pp 1799-1810. https://doi.org/10.1016/j.istruc.2022.08.102

Hatzigeorgiou, G.D., Papagiannopoulos, G.A. "Inelastic velocity ratio", Earthquake Eng Struct Dyn, Vol. 41, 2012, pp 25–41. https://doi.org/10.1002/eqe.2172

Hatzigeorgiou, G.D., Beskos, D.E. "Inelastic displacement ratios for SDOF structures subjected to repeated earthquakes", Engineering Structures, Vol. 31(11), 2009, pp 2744–55. https://doi.org/10.1016/j.engstruct.2009.07.002

Hatzigeorgiou, G.D., Pnevmatikos, N.G. (2014) Maximum damping forces for structures with viscous dampers under near-source earthquakes. Engineering Structure, Vol. 68, 2014, pp 1–13. http://dx.doi.org/10.1016/j.engstruct.2014.02.036

Kam, W.Y., Pampanin, S., Palermo, A., Carr, A.J. "Self-centering structural systems with combination of hysteretic and viscous energy dissipations", Earthquake Engineering and Structural Dynamics, Vol.39 (10), 2010, pp 1083–1108. https://doi.org/10.1002/eqe.983

Konstandakopoulou, F., Hatzigeorgiou, G. "Constant-ductility inelastic displacement, velocity and acceleration ratios for systems subjected to simple pulses", Soil Dyn Earthquake Eng, Vol.131, 2020, pp 106027. https://doi.org/10.1016/j.soildyn.2019.106027

Obando, J.C., Lopez-Garcia, D. "Inelastic displacement ratios for nonstructural components subjected to floor accelerations" Journal of Earthquake Engineering, 2016, pp 1–26. https://doi.org/10.1080/13632469.2016.1244131

Pardalopoulos, S.I., Pantazopoulou, S.J. "Seismic response of nonstructural components attached on multistorey buildings", Earthq Eng Struct Dyn, 2015, Vol. 44(1), pp 139–58. https://doi.org/10.1002/eqe.2466

Pisal, A.Y., and Jangid, R.S. "Dynamic response of structure with tuned mass friction damper", Int J Adv Struct Eng, Vol. (8), 2016, pp 363–377. https://doi.org/10.1007/s40091-016-0136-7

Ruiz-García, J. "Inelastic displacement ratios for seismic assessment of structures subjected to forward-directivity near-fault ground motions", Journal of Earthquake Engineering, 2011, Vol. 5, pp 449–68.

SeismoSignal, version 4.3.0, Pavia, Italy: Seismosoft Ltd. Retrieved from http://www.seismosoft.com/en/HomePage.aspx

Soni, D.P., Mistry, B.B., Jangid, R.S., and Pancha, V.R. "Seismic response of the double variable frequency pendulum isolator", Structural Control and Health Monitoring, Vol. (18), 2011, pp 450–470. https://doi.org/10.1002/stc.384

Yaghmaei-Sabegh، S., Daneshgari, S., Neekmanesh, S. "Inelastic displacement ratio for high damping SDOF systems built on soft soil sites", Soil Dynamics, and Earthquake Engineering, Vol. 135, 2020, pp 106203. https://doi.org/10.1016/j.soildyn.2020.106203

Disclaimer